

Copyright © 2010 IEEE

Reprinted from

Proceedings IEEE Topical Meeting on Silicon Monolithic Integrated Circuits in RF Systems (SiRF 2010), New Orleans, LA, USA, Jan. 11 - 13, 2010, S. 21 – 24

This material is posted here with permission of the IEEE. Such permission of the IEEE does not in any way imply IEEE endorsement of any of Universität Ulm's products or services. Internal or personal use of this material is permitted. However, permission to reprint/republish this material for advertising or promotional purposes or for creating new collective works for resale or redistribution must be obtained from the IEEE by writing to pubs-permissions@ieee.org.

By choosing to view this document, you agree to all provisions of the copyright laws protecting it.

Impulse Generator Targeting the European UWB Mask

Bernd Schleicher and Hermann Schumacher

Ulm University, Institute of Electron Devices and Circuits, Albert-Einstein-Allee 45,
89081 Ulm, Germany, phone: +49-731-5031593, e-mail: bernd.schleicher@uni-ulm.de

Abstract—This paper presents a monolithic impulse generator IC targeting the spectral mask for ultra-wideband applications allocated in the European Union. The multicycle impulse is based on a spike triggered resonant circuit and has a peak to peak output amplitude of 32 mV and a time domain extension of 0.83 ns (full width at half maximum). It can generate single pulses as well as repetition rates exceeding the 200 MHz shown in this paper. The IC includes a conversion stage, which can generate the triggering spike from a low slew rate signal. The IC is fabricated in a Si/SiGe HBT production technology, has a power consumption of 58.6 mW at 200 MHz repetition rate and an on-chip area of $480 \times 880 \mu\text{m}^2$, both including the conversion stage. Based on the time domain measurement a model of the impulse transient for the use in system simulations is also presented. The model equation applies a summation of two Gaussian bell shapes as the envelope function, which is multiplied with a phase-corrected sinusoidal waveform to arrive at the final shape.

Index Terms—Impulse generator, impulse-radio ultra-wideband, IR-UWB, European UWB mask.

I. INTRODUCTION

Impulse generators are the core component of any impulse-radio ultra-wideband (IR-UWB) transmission system. They are used in the transmitter for both energy detection and correlation-type systems and are defining the spectral emission characteristics. Impulse generators published up to now are typically targeting the ultra-wideband spectral masks allocated by the Federal Communications Commission (FCC) in 2002 [1]. Some approaches are intended to make efficient use of the complete mask, e. g. [2]–[4], while other approaches are suggesting to divide the FCC mask in two bands, separated by the W-LAN band around 5.2–5.8 GHz. For the latter approach, impulse generators targeting the lower band were demonstrated in e. g. [5], [6] and targeting the higher band in e. g. [7]. Another concept, presented for example in [8], generates impulses radiating in subbands with a width of 528 MHz in the lower part of the FCC mask.

In 2007 the Electronic Communications Committee (ECC, a committee of the Conference of Postal and Telecommunications Administrations (CEPT) in Europe) allocated as well in Europe a frequency band for unlicensed use of ultra-wideband communications and radar systems [9]. This mask allows a maximum mean effective isotropic radiated power (EIRP) density of -41.3 dBm/MHz from 6–8.5 GHz. The signal level below 6 GHz should be attenuated by 28.7 dB to -70 dBm/MHz and above 8.5 GHz

by 23.7 dB to -65 dBm/MHz . Fig. 1 shows the allowed power spectral densities (PSD) vs. frequency, and the FCC indoor mask for comparison. The band from 4.2–4.8 GHz is not considered here, because its allocation is time limited and will change to the shown PSD by the end of 2010.

When calculating the power available in the bandwidth (BW) from 6–8.5 GHz, we obtain

$$P = 10^{PSD/10} \cdot BW = 0.185 \text{ mW} . \quad (1)$$

This is the maximum power an impulse can have, making best use of the rectangular shape of the mask. A drawback of using such an impulse with an almost rectangular spectral envelope is that it would have an extremely long time domain response, allowing only very low data rates. Therefore the European frequency allocation requires adequate impulse shapes and impulse generating concepts, which on the one hand make efficient use of the mask, and on the other hand show an adequately short time domain duration. In this paper an impulse generator is presented, which shows a concept to fulfill these requirements and is to the best of the authors' knowledge the first impulse generator IC targeting the European UWB mask.

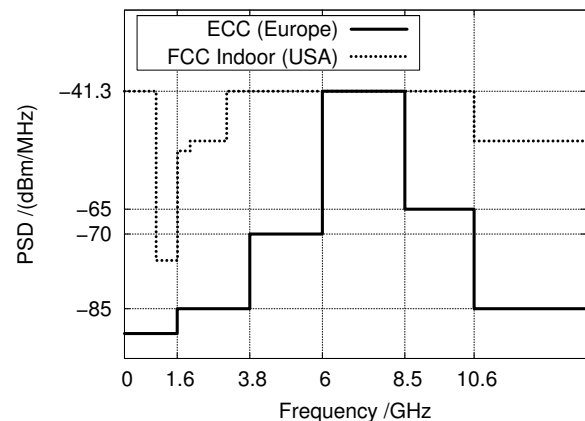


Fig. 1. The European UWB mask compared to the FCC indoor mask.

II. SI/SiGe HBT TECHNOLOGY

The circuit is realised in the $0.8 \mu\text{m}$ Si/SiGe heterojunction bipolar transistor (HBT) production technology supplied by Telefunken Semiconductors, Heilbronn, Germany

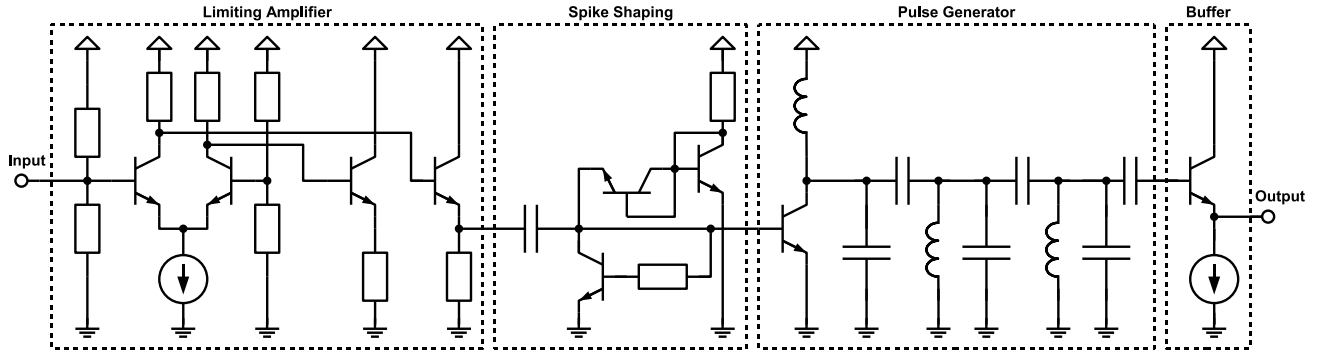


Fig. 2. Simplified circuit schematic of the impulse generator. Only part of the bias arrangement is shown here.

[10]. It has two kinds of vertical npn transistors; the transistors without selectively implanted collector (non-SIC) have a maximum frequency of oscillation $f_{\max} \approx 90$ GHz and a transit frequency $f_T = 50$ GHz at a collector-emitter breakdown voltage $BV_{CEO} = 4.3$ V, whereas the transistors with selectively implanted collector (SIC) have a $f_{\max} \approx 90$ GHz and $f_T = 80$ GHz at $BV_{CEO} = 2.4$ V. The technology has a $0.8 \mu\text{m}$ feature size and a minimum effective emitter size on wafer for vertical npn HBT transistors of $0.5 \times 1.1 \mu\text{m}^2$. The technology provides four types of resistances, MIM and nitride capacitances and a three layer metal system. The spiral inductors are located in the top metal layer with the underpass in the metal layer below. The IC was fabricated on a standard low-resistivity $20 \Omega\text{cm}$ silicon substrate.

the simplified circuit schematic of Fig. 2. The first function block contains two limiting amplifier stages, where only one is shown in Fig. 2. They are used to increase the risetime of the incoming triggering signal. Two limiting amplifier stages are used to make the risetime at the output of this block widely independent from the risetime of the incoming signal, so a signal with a low slew-rate (e.g. a sinusoidal signal) can be used as input control signal. Such a preparation of the input signal is missing in many impulse generation concepts, but comes along with a higher power consumption. The first stage of the limiting amplifier operates at a supply voltage of 3 V, while the second limiting amplifier requires a 4.5 V supply.

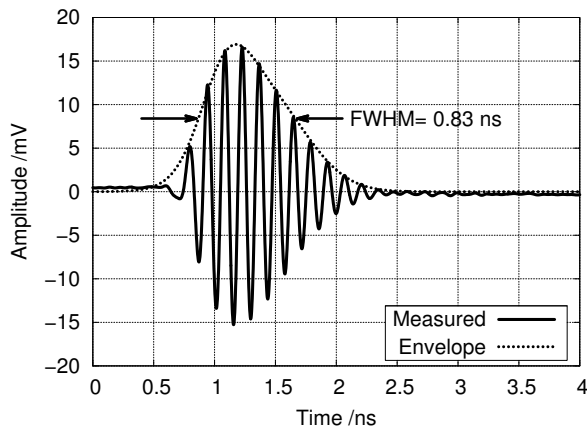


Fig. 3. Measured time domain output waveform of the impulse generator.

III. CIRCUIT CONCEPT

The circuit idea is similar to the concept presented in [11], but the LC series resonance circuit used there for pulse shaping is replaced by a more complex structure using coupled LC resonators, due to the higher required quality factor of the pulse shaper. The circuit can be divided into four main function blocks, as can be seen in

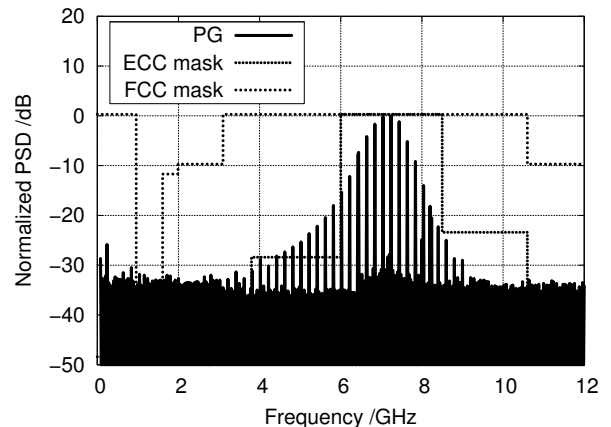


Fig. 4. Measured normalised spectral power density in a 1 MHz measurement bandwidth of the impulse generator at a repetition rate of 200 MHz compared to the FCC and the ECC spectral masks.

The rectangular output signal of the limiting amplifiers is fed to the second function block. There, a spike, shaped like a Gaussian impulse, is generated from the rising slope of the rectangular signal, while it suppresses the negative spikes originating from the falling slope. The Gaussian shaped spikes are fed into the function block for impulse generation, where a relaxation oscillation is induced in

a triple-circuit capacitively coupled bandpass filter. The bandpass filter was adjusted to have a center frequency in the middle of the ECC mask and a bandwidth which ensures compliance with the mask. A triple-circuit bandpass filter was found to be necessary to provide the necessary quality factor for the narrow ECC mask. In each LC-resonator stage the resonating frequency needs to be the same, otherwise the beat frequency between the resonators distorts the time domain output waveform and leads to a ringing, which would increase the impulse width. To this end, the individual inductance and capacitance values are adjusted in simulation, taking the reactive components of source and load impedance into account.

The last function block consists of a buffer stage, which is used to drive a $50\ \Omega$ load.

IV. MEASUREMENT RESULTS

The circuit is characterized on-wafer using a signal source with a 200 MHz sinusoidal signal at the input of the IC, generating an unmodulated impulse train with a 200 MHz repetition rate at the output. For the time domain characterization a real time oscilloscope with 13 GHz bandwidth is connected to the output of the IC. In Fig. 3 the recorded output waveform of a single impulse can be seen. The generated impulse has a peak to peak amplitude of 32 mV and a time domain extension of 0.83 ns, using the full width at half maximum (FWHM). The FWHM extension is measured using the envelope function of the waveform and is chosen as a measure for the impulse width, because it defines a precisely measurable entity.

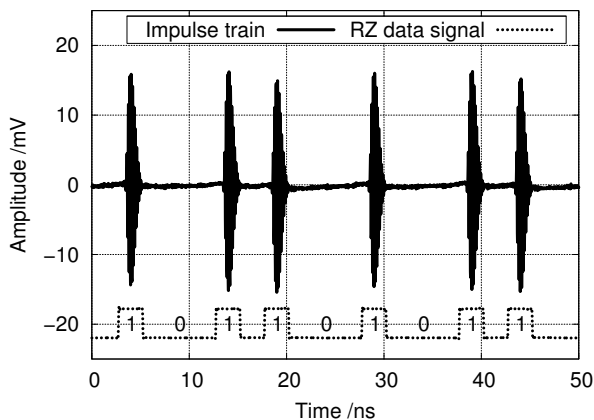


Fig. 5. Measured time domain output waveform of an 200 MBit/s OOK modulated impulse train.

To assess the frequency domain behavior, a spectrum analyzer is connected to the impulse generator output. In Fig. 4 the measured normalised PSD of the unmodulated impulse train with a repetition rate of 200 MHz in a 1 MHz resolution bandwidth is shown. The maximum measured power spectral density is $-44.2\ \text{dBm/MHz}$, albeit for a

compliance check against the maximum allowed EIRP the gain of the transmission antenna, the impulse repetition rate and the modulation type would have to be taken into account. The normalised curve is compared with the normalised European and FCC indoor masks in Fig. 4. It can be seen that the upper part of the impulse fits into the European mask, while the lower part violates the mask at approximately $-15\ \text{dB}$ from the maximum value. In a transmission system this could be adjusted by bandpass filtering, which may be part of the transmit antenna. Compared to an impulse completely filling the mask, the presented impulse shows an implementation loss of 4.4 dB when summing up the power in the band from 6–8.5 GHz, but, as mentioned above, with the advantage of a short time domain duration.

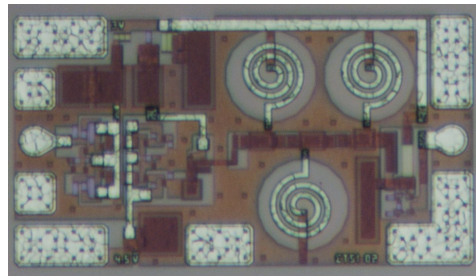


Fig. 6. Micrograph of the monolithic impulse generator circuit. The IC has a size of $480 \times 880\ \mu\text{m}^2$.

In a further measurement the input of the impulse generator is now fed with a return-to-zero (RZ) coded modulation sequence at a repetition rate of 200 MHz. In Fig. 5 the on-off keying (OOK) modulated impulse train and the controlling RZ data signal is shown. With the presented impulse generator, data rates exceeding the 200 MBit/s shown can be achieved - the limitation is the availability of a high-speed bit pattern generator. The complete circuit has a power consumption of 58.6 mW at 200 MHz repetition rate and a size of $480 \times 880\ \mu\text{m}^2$. A micrograph of the fabricated IC can be seen in Fig. 6.

V. MODELLING THE IMPULSE SHAPE

For system simulations using the presented impulse shape an equation-based modelling of the transient waveform is necessary. This can be done by a sinusoidal signal windowed by an envelope function. Here an envelope consisting of the summation of two Gaussian shaped functions is suggested, which accounts for the unsymmetric rise and falltime of the impulse. Each Gaussian function has the form

$$G_{1,2}(t) = a_{1,2} \cdot e^{-((t-b_{1,2})/c_{1,2})^2}, \quad (2)$$

where the coefficients a , b and c are defining amplitude, position and width of each of the two Gaussian functions, respectively. The complete proposed function for

modelling the impulse shape contains the summation of the exponential functions and is multiplied with a phase-corrected sinusoidal signal. It can be written as

$$y(t) = (G_1(t) + G_2(t)) \cdot \sin(2\pi f \cdot (t + \tau/f)) , \quad (3)$$

where f is the center frequency of the impulse and τ defines the phase correction. The phase correction factor is necessary for a coherent transmission of the impulses. The values for the coefficients were found by careful fitting to the normalized time domain impulse shape.

TABLE I
FITTED COEFFICIENTS FOR THE MODELLED FUNCTION

	a	b /ns	c /ns	f /GHz	τ
G_1	0.5	0.85	0.29	7.12	0.12
G_2	0.66	1.15	0.5		

Tab. I provides the fitted coefficients for the normalized measured time domain impulse, while Fig. 7 compares the modelled curve with the measured curve. Furthermore, the two Gaussian functions and the envelope function can be seen in Fig. 7.

VI. CONCLUSION

In this paper an impulse generator IC has been shown targeting the ECC UWB mask with a multicycle impulse shape. The time domain waveform has a peak to peak amplitude of 32 mV and a FWHM of 0.83 ns. It has been shown that the previously demonstrated concept of using a spike-triggered on-chip resonant circuit can be extended to meet the narrower ECC mask. The selectable repetition frequency for the presented impulse generator can be adjusted very flexible between DC and exceeding the 200 MHz shown in these experiments. It has been shown furthermore that the measured impulse shape can be accurately modeled using two Gaussian functions and a sinusoidal function. This model can be easily adopted to waveforms with similar shape but different width and spectral location.

ACKNOWLEDGMENT

The authors are indebted to the SiGe foundry of Telefunken Semiconductors, Heilbronn, Germany for fabrication of the IC. This work is funded by the German Research Foundation (DFG) by means of the priority programme UKoLoS. For more information visit: <http://www.emt.tu-ilmenau.de/ukolos>.

REFERENCES

[1] Federal Communications Commission, "Revision of Part 15 of the Commission's Rules Regarding Ultra-Wideband Transmission Systems," FCC, Washington, D.C., USA, First report and order 02-48, April 2002.

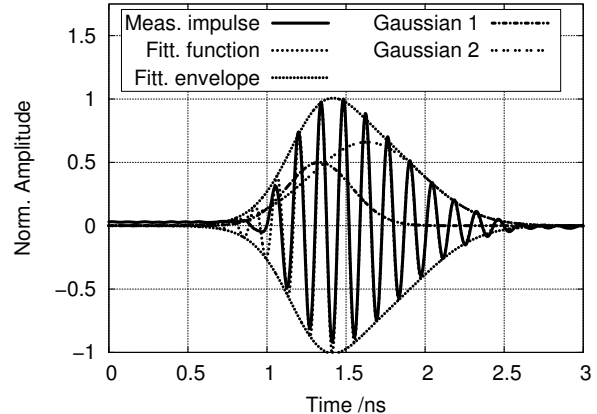


Fig. 7. Comparison of normalised measured and fitted time domain output waveform, including the envelope functions and the two Gaussian functions used to build the envelope function.

[2] Y. Bachelet, S. Bourdel, J. Gaubert, G. Bas, and H. Chalopin, "Fully integrated CMOS UWB pulse generator," *Electronics Letter*, vol. 42, no. 22, pp. 1277 – 1278, October 2006.

[3] J. Dederer, B. Schleicher, F. de Andrade Tabarani Santos, A. Trasser, and H. Schumacher, "FCC compliant 3.1-10.6 GHz UWB Pulse Radar System using Correlation Detection," in *IEEE MTT-S International Microwave Symposium (IMS)*, Honolulu, Hawaii, USA, June 2007.

[4] A. Cacciatori, L. Lorenzi, and L. Colalongo, "A Power Efficient HBT Pulse Generator for UWB Radars," in *IEEE International Symposium on Circuits and Systems (ISCAS)*, New Orleans, LA, USA, May 2007, pp. 3916–3919.

[5] T. Norimatsu, R. Fujiwara, M. Kokubo, M. Miyazaki, A. Maeki, Y. Ogata, S. Kobayashi, N. Koshizuka, and K. Sakamura, "A UWB-IR Transmitter With Digitally Controlled Pulse Generator," *IEEE J. Solid-State Circuits*, vol. 42, no. 6, pp. 1300–1309, June 2007.

[6] L. Xia, Y. Huang, and Z. Hong, "Low power amplitude and spectrum tunable IR-UWB transmitter," *Electronics Letter*, vol. 44, no. 20, pp. 1200–1201, September 2008.

[7] S. Sim, D.-W. Kim, and S. Hong, "A CMOS UWB Pulse Generator for 6-10 GHz Applications," *IEEE Microwave Wireless Compon. Lett.*, vol. 19, no. 2, pp. 83–85, February 2009.

[8] A. T. Phan, J. Lee, V. Krizhanovskii, Q. Le, S.-K. Han, and S.-G. Lee, "Energy-Efficient Low-Complexity CMOS Pulse Generator for Multiband UWB Impulse Radio," *IEEE Trans. Circuits Syst.*, vol. 55, no. 11, pp. 3552–3563, December 2008.

[9] Electronic Communications Committee (ECC) within the European Conference of Postal and Telecommunications Administrations (CEPT), "Commission decision of 21 February 2007 on allowing the use of the radio spectrum for equipment using ultra-wideband technology in a harmonised manner in the Community," Official Journal of the European Union, document number C(2007) 522, Feb. 2007.

[10] A. Schüppen, J. Berntgen, P. Maier, M. Tortschanoff, W. Kraus, and M. Averweg, "An 80 GHz SiGe production technology," *III-Vs Review*, vol. 14, no. 6, pp. 42–46, August 2001.

[11] J. Dederer, C. Schick, A. Trasser, and H. Schumacher, "A SiGe Impulse Generator for Single-Band Ultra-Wideband Applications," *Semiconductor Science and Technology*, vol. 22, pp. 200–203, December 2006.